



Republic of Iraq
Ministry Of Higher Education and
Scientific Research
University of Babylon
College of Science
Department of Physics



Project of Research

**Calibration Relation of TDLS Spectrometer to Measure A Gas Concentration
of Some Gasses Using Saw Tooth Wave Signal**

علاقة معايرة مطياف TDLS لقياس تركيز الغاز لبعض الغازات باستخدام إشارة موجة سن المنشار

By Student

Zainab Hussain Nasser

B.Sc. physics

Scholar year 2023-2024

Supervised by

Asst. Prof. Dr. Samira Adnan Mahdi

بِسْمِ اللَّهِ الرَّحْمَنِ الرَّحِيمِ

(وَيَسْأَلُونَكَ عَنِ الرُّوحِ ۗ قُلِ الرُّوحُ مِنْ أَمْرِ رَبِّي وَمَا أُوتِيتُمْ مِنَ
الْعِلْمِ إِلَّا قَلِيلًا)

صدق الله العلي العظيم

(سورة الإسراء : آية 85)

Supervisor Certification

I certify that the research topic titled (Calibration Relation of TDLS Spectrometer to Measure A Gas Concentration of Some Gasses Using Saw Tooth Wave Signal) and completed by the student (Zainab Hussain Nasser) was conducted under my supervision in the Department of Physics / College of Science / University of Babylon as a partial requirement for obtaining a Bachelor's degree in Physics for the period 1/10/ 2023 until 5/1/2024.

Signature:

Assist. Prof. Dr. Samira Adnan Mahdi

Date: / / 2024

Acknowledgments

I extend my sincere thanks to my professors in the Department of Physics, grateful for their help, advice, and moral support throughout the university career that I spent, asking God Almighty to preserve and guide them and make them an asset for future generations of students. Assist. Prof. Dr. Samira Adnan Mahdi is the owner of high morals, kind words, wonderful advice, and abundance of knowledge. I thank him for helping us in completing our graduate research.

Abstract

This research investigates the establishment of a calibration relation for a Tunable Diode Laser Spectrometer (TDLS) designed to quantify ammonia (NH₃) gas concentration. The system utilizes a sawtooth wave modulation technique to enhance signal-to-noise ratio and improve measurement accuracy. A controlled environment with known NH₃ concentrations is employed to generate a robust calibration curve correlating the measured TDLS signal to actual gas concentration.

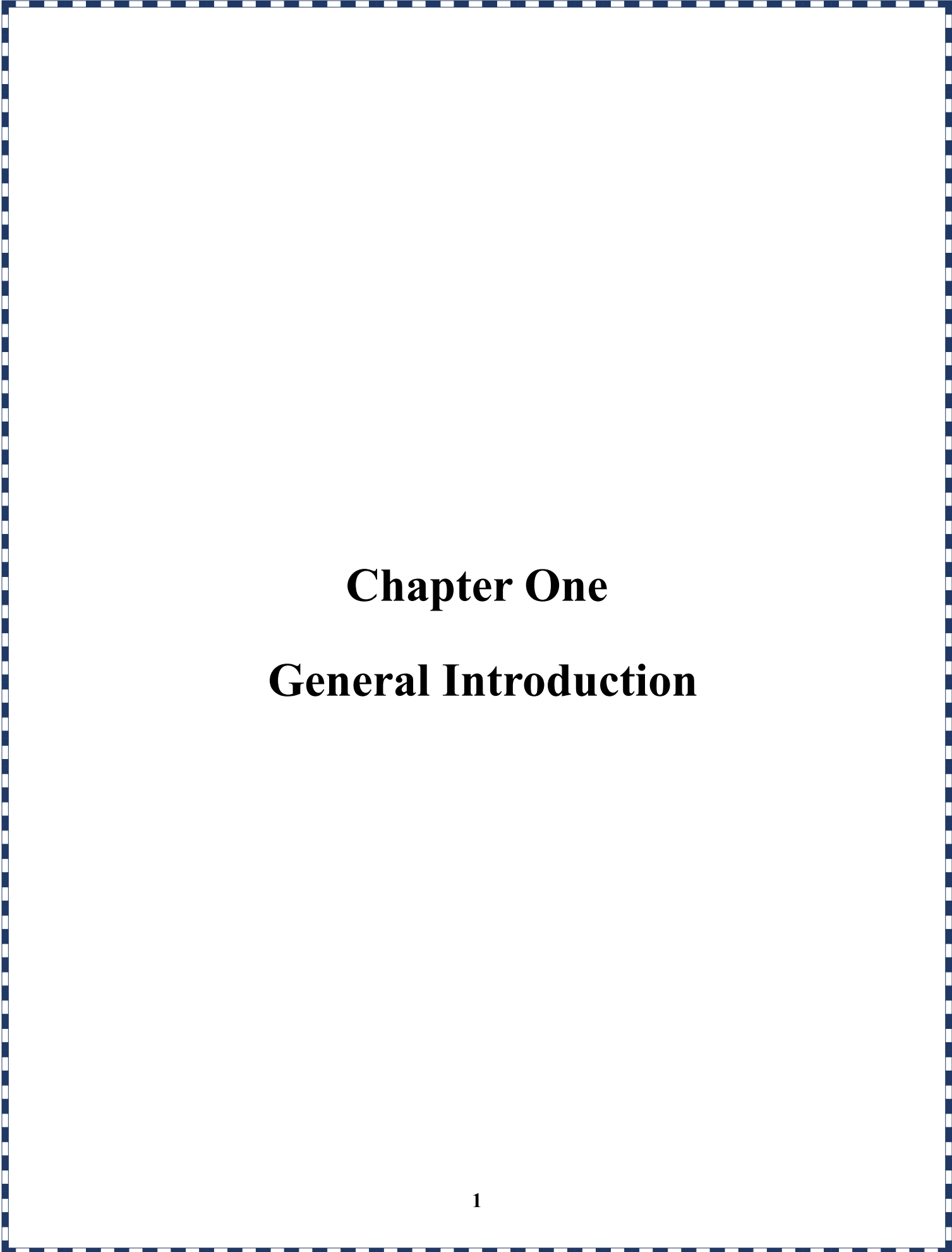
The study focuses on evaluating the linearity of the TDLS signal response across a range of NH₃ concentrations, determining the system's sensitivity to detect minute changes in gas levels, and assessing the stability and repeatability of measurements under varying conditions. The influence of sawtooth wave parameters, such as frequency and amplitude, on the calibration curve and measurement accuracy is also analyzed. Through rigorous experimentation and data analysis, the research aims to optimize the sawtooth wave modulation technique and establish a reliable calibration curve for precise NH₃ quantification.

This research contributes to the advancement of TDLS technology for accurate and reliable gas sensing applications. The developed calibration relation serves as a crucial reference for converting measured TDLS signals into actual NH₃ gas concentrations, enabling effective monitoring and control of NH₃ emissions in various industrial and environmental settings. By exploring the intricacies of sawtooth wave modulation and its impact on measurement accuracy, this study provides valuable insights for optimizing TDLS system performance and expanding its applicability in diverse gas sensing scenarios.

Table Contents

Chapter One: General Introduction	1
1.1 Introduction to Spectroscopy	2
1.2 Spectrometer	3
1.3 Open-Path Spectroscopy.....	4
1.4 Types of Open-Path Spectroscopy.....	6
1.4.1 Ultraviolet Differential Optical Absorption Spectroscopy (UV-DOAS).....	6
1.4.2 Fourier Transform Infrared (FT-IR)	6
1.4.3 Tunable Diode Laser Spectroscopy (TDLS).....	7
1.5 Internal Circuit of TDL.....	8
1.6 Applications of Open-Path Spectroscopy.....	9
1.7 Ammonia (NH ₃).....	9
1.7.1 Physical Properties of Ammonia	10
1.7.2 Chemical Properties of Ammonia (NH ₃).....	12
1.8 Literature Survey	15
Chapter Two: Theoretical Method	18
2.1 The Mathematical Description of Sawtooth with Superimposed Sine Wave .	19
2.2 The Mathematical Description of Sinusoidal Wave with A Step Function Offset.....	19
2.3 Simulations of Sawtooth with Superimposed Sine Wave	20

2.4 Simulation Results of Sawtooth with superimposed sine wave	21
2.4.1 With no noise	21
Chapter Three: Results and Discussion	22
3.1 Results	23
Chapter Four: Conclusions	28
References	30



Chapter One

General Introduction

1.1 Introduction to Spectroscopy

We perceive the world via the interaction of visible light with the light receptors in our eyes. The light is emitted from the sun or from other light sources. It is then reflected from (or transmitted through) the objects in our surroundings. In these processes, the color changes because some of the light is absorbed by the objects. How much and what spectral regions are absorbed depends on the atoms and molecules in these objects. The light not absorbed reaches our eyes. It carries the information of the molecular structure of our surroundings with it.

In our eyes its color is analyzed by 3 different types of photoreceptors which absorb different light in spectral regions. In this way we perform a spectroscopic experiment every time we look at things. There is a light source, and object that reflects, transmits, scatters and absorbs light and a wavelength dependent detector in our eyes. An apparatus for spectroscopic studies is called spectrometer and a plot of a particular property of matter against wavelength, frequency or energy of radiation is called spectrum.

Not only light but also other types of electromagnetic radiation provide powerful information on biological systems. The study of the interaction of electromagnetic radiation with matter is called spectroscopy. Because of the wave-particle dualism of matter, spectroscopy includes the related study of the interaction between matter and particles - like electrons and neutrons.

With this definition X-ray diffraction neutron scattering, electron microscopy, and NMR are spectroscopic methods. However, we will not discuss these techniques here, because they are covered in the structural biochemistry course. This course deals instead with the following techniques: UV/vis (ultraviolet/visible) spectroscopy, fluorescence, circular dichroism, Raman spectroscopy, Infrared

spectroscopy, and electron spin resonance. Most of these use light in the UV/vis spectral range, infrared spectroscopy uses infrared light and electron spin resonance microwave radiation.

In addition to explaining the fundamentals of these techniques, we will also discuss some of their applications to biological systems and biological processes [1].

1.2 Spectrometer

The basic function of any spectrometer is to take in light, break it into its spectral components, digitize the signal as a function of wavelength, and read it out and display it via a computer. In the first step of this process, light is directed through a fiber optic cable into the spectrometer through an entrance slit, which is a narrow aperture.

The slit vignettes the light as it enters the spectrometer. Then, in most spectrometers, the divergent light is collimated by a concave mirror and directed onto a grating. Following this, the grating disperses the spectral components of the light at slightly varying angles.

The light is then focused by a second concave mirror and imaged onto the detector. Alternatively, all of the three functions can be simultaneously performed using a concave holographic grating.

Once the light is imaged onto the detector, the photons are converted into electrons. These electrons are digitized and read out through a USB (or serial port) to a computer.

Based on the number of pixels in the detector and the linear dispersion of the diffraction grating, the software interpolates the signal to generate a calibration that

enables the data to be plotted as a function of wavelength over the given spectral range. This data can be subsequently used and manipulated for many spectroscopic applications [2].

1.3 Open-Path Spectroscopy

Open-path spectroscopy is known for its ability to provide real-time measurements of dozens of compounds over sampling paths of up to 1000 meters in length. Advances in open-path monitoring technology and data processing techniques, coupled with new regulatory requirements, have greatly increased the acceptance and widespread application of spectroscopy-based open-path measurements. Large industrial facilities adjacent to residential communities are a particular application of interest, because traditional fixed-point analyzers lack the spatial coverage of the open-path instruments. Open-path analyzers include ultraviolet differential optical absorbance spectroscopy (UV-DOAS), Fourier transform infrared (FT-IR), and tunable diode laser (TDL) technologies [3].



Figure (1.1): Open-path spectrometer

Open-path analyzers measure absorbance of airborne compounds between a light source and a detector. Different compounds have unique absorbance characteristics at discrete wavelengths which correspond to absorption spectra when scanning over a range of wavelengths. The agreement between measured spectra and reference spectra (the spectral match) is used to identify compounds present. Quantification is achieved by scaling of the reference spectra. The appropriate open-path analyzer is selected based on the absorbance wavelengths of the compounds of interest.

A monostatic configuration uses a combined light source and detector at one end of the open sampling path and a reflector located

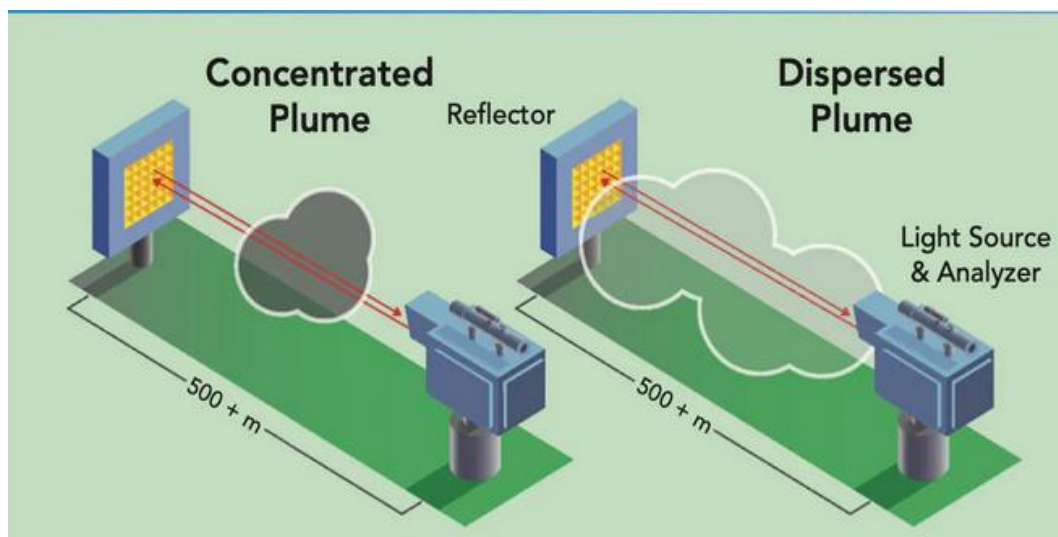


Figure (1.2): Monostatic configuration

. **Figure (1.2)** shows an example of a monostatic configuration. A bistatic system has the light source and detector on opposite sides of the path, across a single path. Importantly, while an open-path system can measure compounds over a large distance (500+ meters), it cannot distinguish between a concentrated or dispersed plume within that path[3].

1.4 Types of Open-Path Spectroscopy

Differences between open-path spectroscopy techniques are primarily due to the light source used, which subsequently determines the available wavelengths for measuring compounds.

1.4.1 Ultraviolet Differential Optical Absorption Spectroscopy (UV-DOAS)

UV-DOAS analyzers contain an ultraviolet (UV) light source—commonly a xenon or deuterium lamp, operating in the range of 225 nm to 400 nm. Target compounds for UV-DOAS analyzers include air toxics such as benzene, toluene, ethylbenzene, xylenes, and sulfur dioxide. This instrument simultaneously measures multiple compounds in real time at a time resolution as fast as every 30 sec. Detection limits are down to low ppb and, in some cases, sub-ppb levels. Typically, one-way path lengths range from 300–700 meters for monostatic configurations, and up to 1000 meters for bistatic configurations[4].

1.4.2 Fourier Transform Infrared (FT-IR)

FT-IR analyzers contain an infrared laser operating in the wavelength range of 670 cm^{-1} to 4400 cm^{-1} at a resolution of 0.5 cm^{-1} . Target compounds for FT-IR analyzers primarily include short-chain hydrocarbons, methane, aldehydes, ammonia, hydrogen cyanide, and other volatile organic compounds (VOCs). FT-IR analyzers can be used to measure multiple compounds simultaneously in real time at a time resolution of approximately once every two to three minutes. Similar to UV-DOAS, typical one-way path lengths range from 300–700 meters for monostatic configurations. Bistatic configurations are not typically used for FT-IR[4].

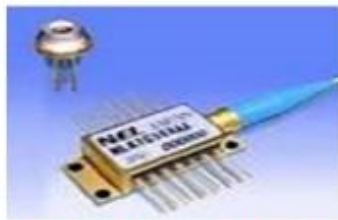
1.4.3 Tunable Diode Laser Spectroscopy (TDLS)

Tunable diode laser (TDL) technology uses a diode laser that emits a narrow wavelength of light tuned to a specified range of interest, which is typically in the mid-IR spectrum. This technique is typically used to measure a single compound of interest, with one or two additional compounds (such as water or methane) measured to verify operations under normal ambient conditions. Example compounds measured by this instrument include hydrogen sulfide, hydrogen cyanide, and hydrogen fluoride[4].

Table (1.1): Considerations for selecting an open-path technology for hydrogen sulfide(H₂S) monitoring

Open-Path Technology	H₂S Selectivity	H₂S MDL (300m path)	Time Resolution	Single or Multiple Gas Combability	Relative Cost
UV-DOAS	Poor	n/a	30 second	multiple	\$\$
FT-IR	Good	1500 ppb	3 minutes	multiple	\$\$\$
TDLS	Best	25 ppb	5 minutes	single	\$

1.5 Internal Circuit of TDL



<http://www.directindustry.com/product-electronics/dfb-laser-diodes-35545-221808.html>

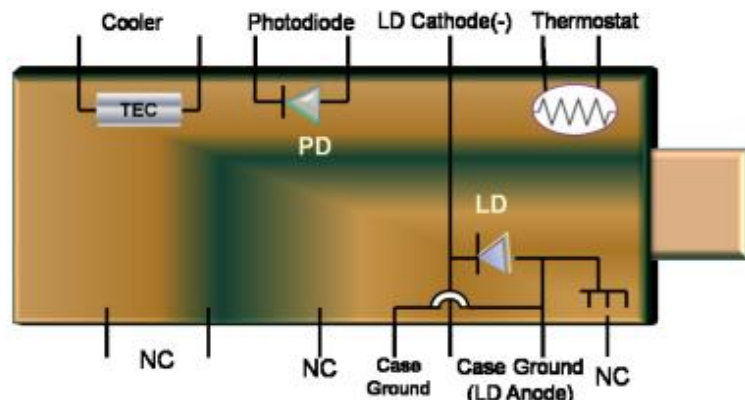


Figure (1.3): Near-infrared tunable diode laser: package picture of TDL (left), internal circuit of TDL (NLK1655STG) (right).

Figure (1.3a) present the 14-pin package of the diode laser. **Figure (1.3b)** shows the internal structure of this package. The main device is an InGaAsP commercial Distribution Feed Back (DFB) butterfly (NLK1655STG) Laser Diode (LD), with (1m) pigtail fiber optics. The central wavelength is 1543 nm, and the fiber optic output power is 26.8 (mW). They lase by applying forward current exceeding threshold values $I_{th} = 17$ mA, $T = 22$ C°. The internal circuit of the butterfly DFB also has An InGaAs PIN monitoring Photo Diode (PD). In this work, this PD is called the internal photodiode and it is monitored to measure the 1/f noise spectrum that is generated by the laser light. The PD is mounted with a tin-lead solder at around 400 picometer from the rear facet of the laser with an angle of 30" to prevent optical feedback in the laser cavity. The temperature of the diode laser is monitored with a thermistor in the butterfly package. A Peltier cooler is used to control the temperature of the laser. All these components are housed in a 14 pin Package

1.6 Applications of Open-Path Spectroscopy

- In municipal waste incinerators.
 - In coal-fired power plants.
 - In the metal industry.
 - Measurement of oxygen in coke oven gas.
 - Increasing efficiency and safety in aluminum smelters.
 - In chemical / oil & gas.
 - Identification and characterization of homopolymers, copolymers, or polymer composite.
 - Pharmaceutical sciences for compound quantification.
- Quantitative analysis. [5].

1.7 Ammonia (NH₃)

Ammonia is an inorganic chemical compound of nitrogen and hydrogen with the formula NH₃. A stable binary hydride and the simplest pnictogen hydride, ammonia is a colorless gas with a distinctive pungent smell. Biologically, it is a common nitrogenous waste, and it contributes significantly to the nutritional needs of terrestrial organisms by serving as a precursor to fertilizers. Around 70% of ammonia produced industrially is used to make fertilizers in various forms and composition, such as urea and diammonium phosphate. [6].

Ammonia occurs naturally and is produced by human activity. It is an important source of nitrogen which is needed by plants and animals. Bacteria found in the intestines can produce ammonia. Ammonia is a colorless gas with a very distinct odor. This odor is familiar to many people because ammonia is used in smelling salts, many household and industrial cleaners, and window-cleaning products.

Ammonia gas can be dissolved in water. This kind of ammonia is called liquid ammonia or aqueous ammonia. Once exposed to open air, liquid ammonia quickly turns into a gas. Ammonia is applied directly into soil on farm fields, and is used to make fertilizers for farm crops, lawns, and plants. Many household and industrial cleaners contain ammonia[7].

Ammonia solutions (containing more than 35% but not more than 50% ammonia) appears as a clear colorless liquid consisting of ammonia dissolved in water. Corrosive to tissue and metals. Although ammonia is lighter than air, the vapors from a leak will initially hug the ground. Long term exposure to low concentrations or short-term exposure to high concentrations may result in adverse health conditions from inhalation. Prolonged exposure of containers to fire or heat may result in their violent rupturing and rocketing.

1.7.1 Physical Properties of Ammonia

Ammonia is a covalent atom, as the dot structure appears to be. Ammonia particle form by the overlap of three hydrogen orbitals and three hybrid sp^3 orbitals of N in the structure as the central atom. A single pair is involved in the fourth sp^3 hybrid orbital. It gives the ammonia particle a trigonal pyramid form. The bond angle of the H-N-H is 107.3° , which is not a tetrahedral angle of $109^\circ 28'$. It is because the bond pair-lone pair repulsions push the N-H bonds slightly inward. In solid and liquid states, ammonia binds by hydrogen bonds[8].



Figure (1.4): Structure of Ammonia (NH₃)

Table (1.2): Lattice parameters of Ammonia

a (Å)	5.193
b (Å)	5.193
c (Å)	5.193
A	90
B	90
Γ	90

Ammonia exhibits classical saturation relationships whereby pressure and temperature are directly related so long as both the vapor and liquid phase are present. It does have a critical pressure and temperature. At atmospheric pressure, a closed container of ammonia vapor and liquid will be in equilibrium at a temperature of -28°F [-33°C]. It should be noted however that if liquid

ammonia is spilled or released to the atmosphere at normal temperatures, the resultant pool of boiling liquid will be significantly colder than -28°F due to the law of partial pressures (the partial pressure of the ammonia vapor in the air near the liquid surface will be less than atmospheric pressure)[9].

Table (1.3): Physical Properties of Ammonia

Property	Value or Detail
Molecular Mass	17.03 g/mol
Colour	Colourless
Odour	Sharp, Intensely Irritating
Physical State	Gas (at room temperature)
Melting Point	-77.7°C
Boiling Point	-33.35°C
Flash Point	11°C
Decomposition Point	500°C
Density (Gas)	0.7710g/L
Density (Liquid)	0.6818g/L
Vapour Density	0.5697 (air has a vapour density of 1)
Critical Temperature	132.4°C
Critical Pressure	111.3 atm
Heat of Fusion	58.1 kJ/mol
Heat of Vaporization	23.3 kJ/mol
Heat of Combustion	-316 kJ/mol

1.7.2 Chemical Properties of Ammonia (NH_3)

Anhydrous ammonia is a naturally occurring compound comprised of two very common elements — nitrogen and hydrogen. The atmosphere is nearly 80% nitrogen, whereas hydrogen is a common element in many organic compounds. This helps to explain why ammonia is a vital chemical in both plant and animal life.

Ammonia is a four-atom molecule comprised of one nitrogen atom and three hydrogen atoms[9].

Ammonia is considered to be a relatively stable compound but this does not mean that ammonia does not participate in any hazardous or potentially hazardous reactions with other materials.

Ammonia reacts readily with a wide variety of substances. Ammonia is incompatible with copper, zinc, or copper-based alloys, and corrosion of these metals will occur.

However, there are journal bearings, thrust washers, and piston rings containing copper bearing materials used within ammonia compressors which are acceptable since they are continually coated with lubricating oil and no degrading chemical reaction occurs. Ammonia is compatible with aluminum, steel, and stainless steels. Certain high tensile strength steels can experience stress corrosion cracking if the ammonia is totally anhydrous. The susceptibility of carbon steels to stress corrosion cracking increases with higher strength steels, particularly in situations with high residual or applied stresses.

The susceptibility to stress corrosion cracking is enhanced when the concentration of oxygen is as low as 0.5 ppm and becomes more inhibited with increasing concentration of water to approximately 0.2%. Ammonia is soluble in water, alcohol, ether, and other organic solvents. It is virtually immiscible with most mineral-based lubricating oils although liquid ammonia will physically carry oil along as it flows[9].

Table (1.4): Chemical Properties of Ammonia[10].

Property	Temperature	Value
pKa	25°C	9.25
Specific heat	0°C	2097.2 J/Kg.K
	100°C	2226.2 J/Kg.K
	200°C	2105.6 J/Kg.K
ΔH_f	0 K	-39,222 KJ/mol
	298 K	-46,222 KJ/mol
Solubility in water, wt%	0°C	42.8 %
	15°C	38 %
	20°C	33.1 %
	30°C	28 %
	40°C	23.4 %
	50°C	18 %
	60°C	14.1 %

1.8 Literature Survey

Peng, Du, and Ding (2020) introduced a novel calibration-free wavelength modulation-direct absorption spectroscopy (WM-DAS) method, integrating DAS absorbance measurement with WMS benefits. In their two-part paper, they detailed theoretical foundations, noise rejection via FFT, and simultaneous fitting for baseline and absorbance. Their experimental validation showcased high accuracy in CO transition analysis, marking significant progress in TDLAS techniques.

Xiaojuan Cui, Fengzhong Dong, and Zhirong Zhang (2017) discussed the increasing need for detecting hazardous gases due to global warming and air quality concerns. Their chapter outlines recent advancements in tunable diode laser absorption spectroscopy (TDLAS), highlighting its sensitivity and applicability in various fields. They also present gas sensors developed by their group, spanning applications from energy and environment to public safety and medical science, reflecting substantial contributions to gas detection technology.

Kevin Duffin, Andrew James McGettrick, Walter Johnstone, and George Stewart (2007) introduced an innovative approach to tunable diode-laser spectroscopy, utilizing inherent phase shifts for signal separation. Their technique enables absolute measurements of gas absorption line shapes, concentrations, and pressures without calibration under defined conditions. Experimental results, including methane absorption measurements, validated the method's accuracy and applicability in industrial settings, showcasing its simplicity, robustness, and suitability for high-temperature environments. This work contributes significantly to advancing gas detection technology.

Steven G. Buckley (2018) explores the evolution, capabilities, and challenges of tunable diode laser absorption spectroscopy (TDLAS), focusing on current techniques and the perennial issue of detecting small absorption dips amid strong laser sources. He discusses the Beer-Lambert law's application, highlighting the limitations imposed by environmental and detector noise. Buckley proposes wavelength modulation as a practical solution, elucidating its implementation and impact on signal strength.

Avishek Guha (2014) focuses on enhancing the application of wavelength modulation with second harmonic detection (WMS-2f) in tunable diode laser absorption spectroscopy (TDLAS) for spatially resolved temperature and concentration reconstructions. They address challenges associated with varying temperature and concentration distributions in flame environments, employing computer tomographic methods to convert line-of-sight measurements into spatially resolved data. Their study includes analysis of reconstruction errors, development of new determination strategies, and benchmarking of 1D and 2D reconstructions.

Deyue Ban, Nan Li, Yongqiu Zheng, and Chenyang Xue (2024) investigated the application of tunable diode laser absorption spectroscopy (TDLAS) combined with Wave Modulation Spectroscopy (WMS) for measuring CO₂ concentrations in flue gas ducts under varying pressure and vibration conditions. Their study identified correlations between pressure, vibration, and measurement accuracy, providing insights into stable gas detection using TDLAS in challenging industrial environments. This research contributes to enhancing monitoring techniques for greenhouse gas emissions from fossil fuel power stations.

Abhishek Upadhyay, David Wilson, Michael Lengden, Arup L. Chakraborty, George Stewart, and Walter Johnstone (2017) present a comprehensive experimental approach to wavelength modulation spectroscopy (WMS) applied to various semiconductor lasers in the near and mid-infrared range. They demonstrate the technique's versatility by extracting gas parameters like nitric oxide, carbon dioxide, and methane concentrations and pressures using different lasers. The study also discusses real-time measurement methodologies and considerations for optimizing laser performance and modulation parameters.

Shan Lin, Jun Chang, Jiachen Sun, and Peng Xu (2022) review advances in tunable diode laser absorption spectroscopy (TDLAS) detection sensitivity. They discuss methods such as absorption line selection, laser improvement, optical path design, data demodulation, and background interference suppression. Summarizing achievements in detecting gases like CH₄, CO₂, and NO, they propose a sensitivity limit hypothesis based on infrared absorption principles, suggesting a theoretical threshold for TDLAS sensitivity enhancement.

Chapter Two

Theoretical Method

2.1 The Mathematical Description of Sawtooth with Superimposed Sine Wave

The mathematical expression which represents the sinusoidal wave with a step function offset can be described by the following equation:

$$i_{in} = p_1 \times t + a \sin (2\pi f_o t) \quad (2-1)$$

where $t = N_{cycle}/f_o$ is the length of the sawtooth function in (sec), $N_{cycle} = 10$ is the number of cycles of a sine wave, $f_o = 500\text{Hz}$ is the modulation frequency of the sine waveform in (Hz), $p_1 = 120 \text{ mA/sec}$ is the slope of the sawtooth function, and $a = 3.5 \text{ mA}$ is the amplitude of the sine wave.

2.2 The Mathematical Description of Sinusoidal Wave with A Step Function Offset

The mathematical expression which represents the sinusoidal wave with a step function offset can be described by the following equation:

$$i_{in} = p_2 \times \frac{t}{p_3} + a \sin (\pi f_o t) \quad (2-2)$$

where, $t = T_N_{cycle}/f_o$ is the total section step period in (sec), $T_N_{cycle} = 100$ is the number of cycles of sine wave that includes in the length step period, $p_2 = 4.5\text{mA}$ is the step offset, and a is the amplitude of the sine wave in (mA), $p_3 = N_{cycles}/f_o$ is the period of the sub-section step function in (sec), $N_{cycles} = 10$ is the number of cycles of a sine wave in one sub-section step period, $f_o = 500 \text{ Hz}$ is the modulation frequency of the sine waveform in (Hz)[11].

2.3 Simulations of Sawtooth with Superimposed Sine Wave

The simulations of light absorption by ammonia gas are based on the Beer-Lambert Law. The fundamental incident intensity of IR light emitted by DFB diode laser was modulated using sawtooth with superimposed sine wave as shown in Eq.2-3.

$$I_0 = [(i_{\text{offset}} - i_{\text{th}}) + p_1 \times t + a \sin (2\pi f_0 t)] \frac{\delta}{\text{area}} \quad (2-3)$$

Where $i_{\text{offset}} = 100$ mA is the DC offset; $i_{\text{th}} = 19$ mA is the threshold current; $a = 3.5$ mA is the amplitude of the sine wave; $p_1 = 120$ mA/sec; $f_0 = 500$ Hz is the modulation frequency; $\delta = 0.2055$ mW/mA is the differential efficiency of the laser current; $\text{area} = 3.1$ mm² is the area of the photodiode. A narrow bandwidth beam of the laser light was generated and swept through the absorption peak of the ammonia gas.

According to the weather conditions on the Martian atmosphere, the pressure is only a few millibars (pressure measurements show a mean pressure of roughly 730 Pa = 7.3 millibar). The measurements were updated by [12].

Doppler broadening dominates and the line-shape of the absorption cross-section becomes Gaussian, in the following simulations the wavelength of the diode laser was modulated by a sawtooth waveform with a superimposed sine wave.

$$\sigma = C e^{-\frac{(w_0 + a \gamma (p_1 \times t + a \sin (2\pi f_0 t)) - w_p)^2}{2\varepsilon^2}} \quad (2-4)$$

If we substitute Eq. (2-3) and Eq. (2-4) in Eq. (2-1) we will get:

$$I = [(i_{\text{offset}} - i_{\text{th}}) + p_1 \times t + a \sin (2\pi f_0 t)] \frac{\delta}{\text{area}} e^{-\beta N L C e^{-\frac{(w_0 + a \gamma (p_1 \times t + a \sin (2\pi f_0 t)) - w_p)^2}{2\varepsilon^2}}} \quad (2-5)$$

I_0 and I (unit: mW/mm²) are the intensity of incident light and transmitted light, respectively; $\beta = 0.355 E^{-17}$ (cm⁻³ /ppm) is the factor to convert the unit from ppm

to cm^{-3} ; N (unit: parts per million) is the gas concentration; and $L = 100$ m is the light path length through the gas. In Eq. 2-3 is the cross-section area of ammonia gas $C = 1\text{E-}20$ cm^2 and its variance nm. Over a wavelength range that is represented by $(w_0 + a \gamma(p_1 \times t + a \sin(2\pi f_0 t)) - w_p)^2$. $w_0 = 1542.8$ nm is the initial value of the scanning wavelength of the diode laser; $p_1 \times t + a \sin(2\pi f_0 t)$ is the sawtooth with superimposed sine wave used to adjust the wavelength of emitted light from the laser; with $a = 3.5$ mA is the amplitude of the sine wave; $\gamma = 0.01$ nm/mA is a modulation factor; $f_0 = 500$ Hz is the modulation frequency; t is time in seconds; and $w_p = 1543.05$ nm is the peak value of the absorption spectrum of ammonia gas.

2.4 Simulation Results of Sawtooth with superimposed sine wave

The simulation procedure of the absorption peak of ammonia gas was performed in two different ways as follows:

2.4.1 With no noise

This section will discuss the results obtained from the simulation process using a sawtooth with superimposed sine waveform to modulate the diode laser current when there is no $1/f$ noise present. The sawtooth function has been proposed in many different gas detection research papers [13], and it realizes a high sensitivity in the TDLS detection system, because the diode laser will tune continuously with a different offset voltage. As a result, the absorption spectrum of ammonia gas will be broader and will include a large absorption area of ammonia gas in the received signal. Therefore, the wavelength of the laser diode will be controlled precisely to obtain the exact and maximum absorption spectrum at individual time interval.

Chapter Three

Results and Discussion

3.1 Results

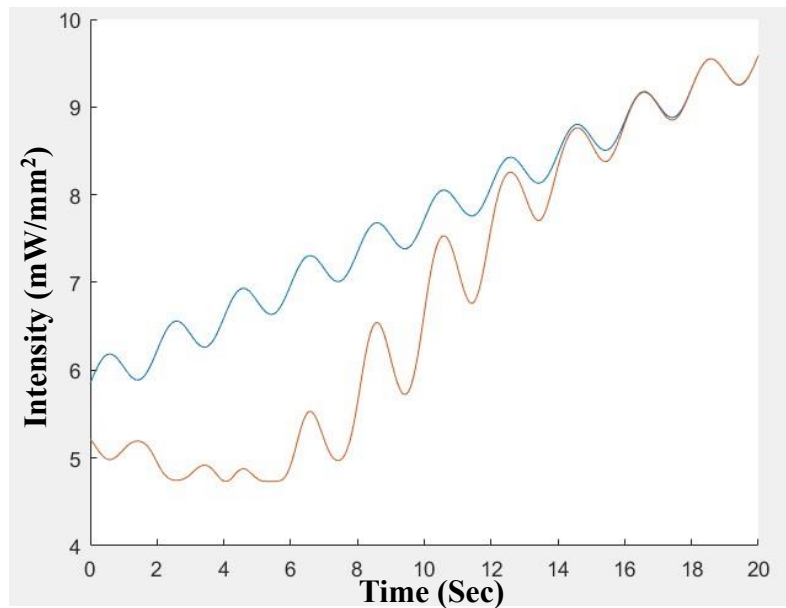


Figure (3.1): The original signal of sawtooth with superimposed sine wave passed through the air (Blue line), and passed through ammonia gas (Red line). The gas concentration 100 ppb.

Figure (3.1) shows the simulated sawtooth with superimposed sine wave with no gas present (Blue line) and with ammonia gas present (Red line). In case of the gas presence (Red line) the amplitude of the sine wave is reduced by the influence of the gas. A nine periods of sine wave were superimposed on top of the sawtooth function, with small amplitude to obtain a broad absorption spectrum of ammonia gas. The absorption spectrum of ammonia gas was obtained at the specific wavelength by simulating Eq. 2-5 as appeared in **Figure (3.1)** inside the ellipse. After obtaining the data in time domain, an FFT was performed in order to analyze the data. The area of the gas absorption peak was then related to the second harmonic of the applied sine wave. A Matlab code was written to find the value of the second harmonic for each

period of a sine wave. Then the relation between the second harmonic and the sine wave number (1-9) in the sawtooth wave was plotted.

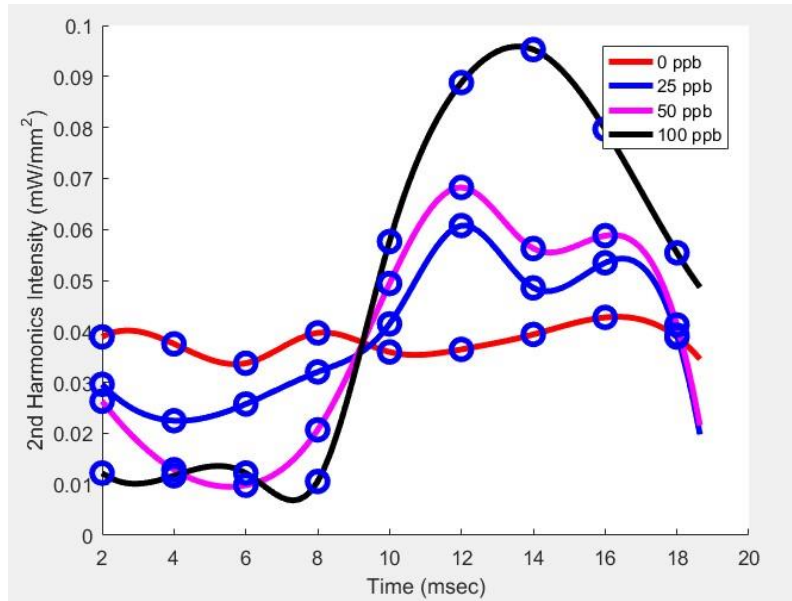


Figure (3.2): The variation of the 2nd harmonic with time (with no noise). One period of sawtooth wave beings at t=2 sec and ends at t = 18 sec. Each point on the curve represents second harmonic calculated from sine wave on sawtooth wave.

When there is no noise present, the relation is nearly symmetric around the 13 seconds as shown in **Figure (3.2)**. That means the amount of the second harmonic value increases gradually until it reaches its highest value, then starts to decline. The most convenient explanation of this behavior of the second harmonic is that the scanning current offset of the diode laser was changing continuously through the sawtooth function. This will increase the value of the emission wavelength of the diode laser until it reaches an appropriate value that can be maximally absorbed by the ammonia gas. After that, the current continues to rise and the wavelength will be

outside of the ammonia absorption spectrum. This will lead to degradation in the value of the second harmonic after 13 seconds.

Figure (3.2) shows the variation of the 2nd harmonic with time (with no noise). One period of sawtooth wave beings at $t=2$ sec and ends at $t = 18$ sec. Each point on the curve represents second harmonic calculated from sine wave on sawtooth wave. The sample data with circle marks, and the fitting curves using the spline method of each gas concentration were plotted in the same plane. Also, the 2nd harmonic has a specific value at zero gas concentration.

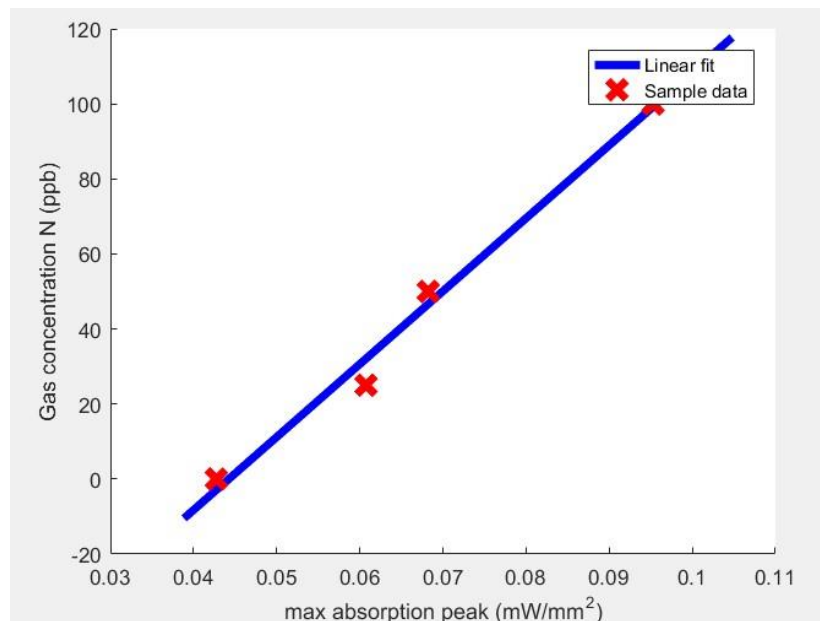


Figure (3.3): Gas concentrations vs. maximum value of 2nd harmonic.

To evaluate the absorption peak of the ammonia gas, several features were extracted from **Figure (3.2)**. For example, the maximum of the 2nd harmonic, and the standard

deviation of all the 2nd harmonic values (9 points). **Figure (3.3)** displays the relation between the maximum of the 2nd harmonic and the gas concentration. The relation is nearly linear. The estimated error in the gas reading was calculated, which represents the difference between the actual gas amount and the estimated value that extracted from the linear fit of the sample data.

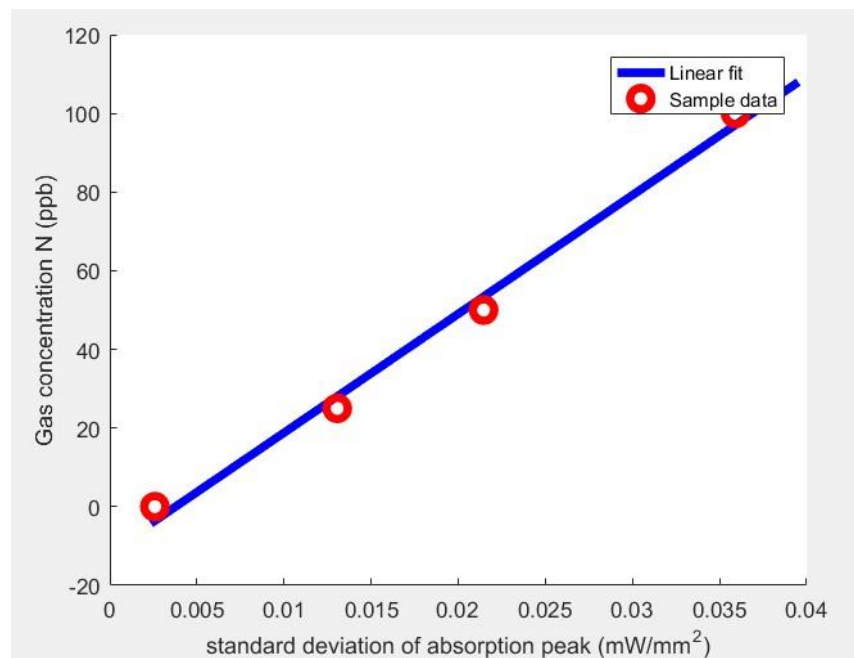


Figure (3.4): Gas concentrations vs. standard deviation of 2nd harmonic values.

The adoption of the standard deviation of the nine values of 2nd harmonic is to reduce the error in the gas concentration readings through the averaging process. Figure 5-5 shows the linear relation between the gas concentration and the standard deviation of the 2nd harmonic values (9 values). The estimated gas concentration was calculated from the linear fit of the sample data points. The estimated error was calculated from the difference between the actual gas value and the estimated value. This calculation was normalized for 100 m laser light path-length.

Chapter Four

Conclusions

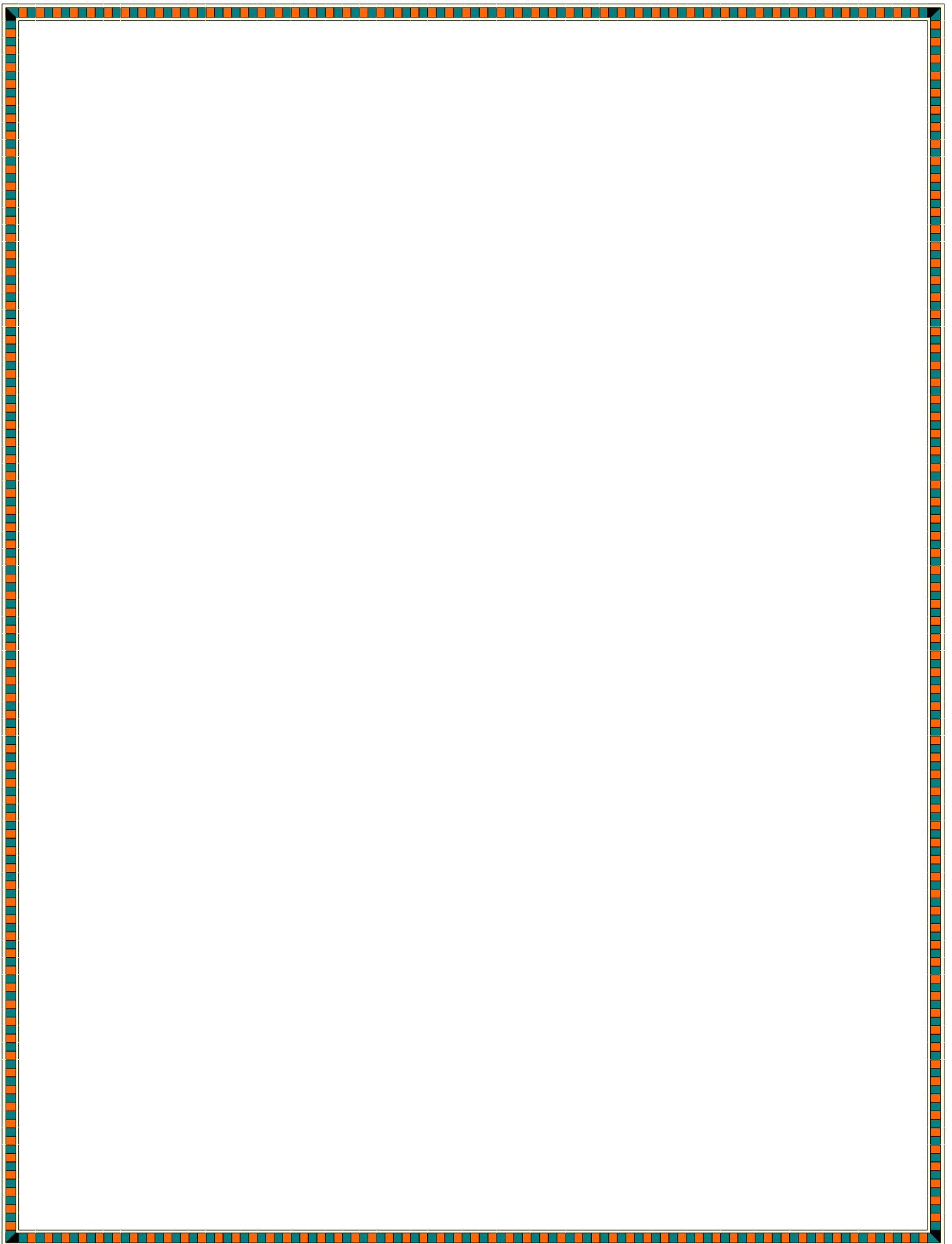
In this work a DSP technique was used by performing a DFFT-BF procedure on the sample data to improve the sensitivity of TDLS spectrometer for gas detection measurements. Several conclusions can be listed in the following steps.

1. The results that were displayed showed that $1/f$ noise has multiple contributing sources, including the injected current and the laser light generated by the diode. The noise profile can determine by the value of α , which should be $1 < \alpha < 2$. α varies with the amount of the current injected into the diode laser. For example, in case of external photodiode, the α value of a 141mA injection current was about 0.9, indicating a strong $1/f$ noise component.
2. The absorption peak of ammonia gas is assumed to have a Gaussian profile, which is true under the assumption a very low pressure so that Doppler broadening occurs. Based on this, the DFFT-BF was performed on the specific number of harmonics which are chosen according to a mathematical procedure (see chapter 4). Because the SFFT of a Gaussian line-shape is also Gaussian, the shape of the DFFT-BF of the absorption signal will not be affected by the DFFT-BF procedure.
3. The simulation and experimental results of ammonia gas measurement using a sine wave modulation waveform agreed with each other. The DFFT-BF procedure reduced the average error in the gas concentration measurements by about 75% compared to the SFFT.
4. The uncertainty in the wavelength value of the diode laser due to $1/f$ noise varies with the injected current of the diode laser. It decreases as the current increase.

References

- [1] “Introduction to Spectroscopy”.
- [2] “The Basic Working Principle of a Spectrometer.” Accessed: Jan. 24, 2024. [Online]. Available: <https://www.azom.com/article.aspx?ArticleID=13364>
- [3] S. R. Schill, R. S. McEwan, R. C. Moffet, J. E. Marrero, C. P. MacDonald, and E. D. Winegar, “Real-World Application of Open-Path UV-DOAS, TDL, and FT-IR Spectroscopy for Air Quality Monitoring at Industrial Facilities,” *Spectroscopy*, pp. 18–22, Nov. 2022, doi: 10.56530/SPECTROSCOPY.QZ5173X6.
- [4] “Air Monitoring Guidelines for Petroleum Refineries AIR DISTRICT REGULATION 12, RULE 15: PETROLEUM REFINING EMISSIONS TRACKING Prepared by the staff of the Bay Area Air Quality Management District,” 2014.
- [5] “Air Monitoring Guidelines for Petroleum Refineries AIR DISTRICT REGULATION 12, RULE 15: PETROLEUM REFINING EMISSIONS TRACKING Prepared by the staff of the Bay Area Air Quality Management District,” 2014.
- [6] “Ammonia Technology Roadmap – Analysis - IEA.” Accessed: Mar. 14, 2024. [Online]. Available: <https://www.iea.org/reports/ammonia-technology-roadmap>
- [7] “Ammonia | Toxic Substances | Toxic Substance Portal | ATSDR.” Accessed: Mar. 14, 2024. [Online]. Available: <https://wwwn.cdc.gov/TSP/substances/ToxSubstance.aspx?toxid=2>
- [8] “What is Ammonia: Structure, Properties, Preparation, Uses.” Accessed: Mar. 14, 2024. [Online]. Available: <https://www.toppr.com/guides/chemistry/amines/ammonia-2/>
- [9] “Ammonia Data Book 2nd Edition - Google Books.” Accessed: Mar. 14, 2024. [Online]. Available: https://www.google.iq/books/edition/Ammonia_Data_Book_2nd_Edition/RE_FMMQAACAAJ?hl=ar

- [10] A. E. Ghaly and K. N. MacDonald, "Development and Testing of an Ammonia Removal Unit from the Exhaust Gas of a Manure Drying System," *Am J Environ Sci*, vol. 9, no. 1, pp. 51–61, Feb. 2013, doi: 10.3844/AJESSP.2013.51.61.
- [11] C. R. Webster *et al.*, "Tunable diode laser IR spectrometer for in situ measurements of the gas phase composition and particle size distribution of Titan's atmosphere," *ApOpt*, vol. 29, no. 7, pp. 907–917, Mar. 1990, doi: 10.1364/AO.29.000907.
- [12] "The weather and climate on Mars for NASA Curiosity rover - The Washington Post." Accessed: Apr. 26, 2024. [Online]. Available: https://www.washingtonpost.com/blogs/capital-weather-gang/post/the-nasa-curiosity-rover-and-weather-on-mars/2012/08/06/a1303d4c-dfdc-11e1-a19c-fcfa365396c8_blog.html
- [13] L. Xiao, C. Li, Q. Li, S. Jia, and G. Zhou, "Low-frequency wavelength modulation spectroscopy with D2 transition of atomic cesium by use of an external-cavity diode laser," *Appl Opt*, vol. 39, no. 6, p. 1049, Feb. 2000, doi: 10.1364/AO.39.001049.





جمهورية العراق
وزارة التعليم العالي والبحث العلمي
جامعة بابل كلية العلوم
قسم الفيزياء



العلاقة المعيارية لمطياف الليزري المتغير لقياس تركيز الغاز لبعض الغازات باستخدام إشارة
أسنان المشط

بحث تخرج للطالب

زينب حسين ناصر

مقدم الى مجلس كلية العلوم في جامعة بابل لنيل شهادة البكالوريوس في علوم الفيزياء

بإشراف

أ. م. د. سميرة عدنان مهدي